European Heart Journal (2005) **26**, 2637–2643
doi:10.1093/eurheartj/ehi496

Clinical research

Correspondence between left ventricular 17 myocardial segments and coronary arteries

Osvaldo Pereztol-Valdés[1], Jaume Candell-Riera[2]*, César Santana-Boado[3], Juan Angel[2], Santiago Aguadé-Bruix[4], Joan Castell-Conesa[4], Ernest V. Garcia[3], and Jordi Soler-Soler[2]

[1] *Departament de Física de la Universitat Autònoma, Barcelona, Spain;* [2] *Servei de Cardiologia, Hospital Universitari Vall d'Hebron, P. del Vall d'Hebron 119-129, 08035 Barcelona, Spain;* [3] *Department of Radiology, Emory University, Atlanta, Georgia; and* [4] *Servei de Medicina Nuclear, Hospital Universitari Vall d'Hebron, Barcelona, Spain*

Received 3 May 2005; revised 22 August 2005; accepted 25 August 2005; online publish-ahead-of-print 23 September 2005

KEYWORDS
Coronary disease;
Scintigraphy;
Angiography;
Angioplasty

Aims The last guidelines recommend a standardized 17-segment model for tomographic imaging of the left ventricle. The aim of this study is to analyse the correspondence of the 17 left ventricular segments with each coronary artery by myocardial perfusion SPECT studies.
Methods and results Fifty patients selected for percutaneous revascularization of one coronary artery [24 left anterior descending (LAD), 15 right coronary artery (RCA), and 11 left circumflex (LCX)] were included. The ^{99m}Tc-labelled compound was injected immediately after the inflation of the balloon during percutaneous coronary angioplasty. At least 90 s of complete occlusion time was required. Maximal contour of regions of hypoperfusion corresponding to each coronary artery occlusion were delineated over the polar map of 17 segments. Nine segments corresponded to only one coronary artery: eight to LAD (basal anterior, basal anteroseptal, mid-anterior, mid-anteroseptal, apical anterior, apical septal, apical lateral, and apex) and one to LCX (basal anterolateral). Basal inferoseptal, mid-inferoseptal, and apical inferior segments could correspond to LAD or RCA. Basal inferior, basal inferolateral, mid-inferior, and mid-inferolateral segments could correspond to RCA or LCX, whereas the mid-anterolateral segment could correspond to LAD or LCX.
Conclusion The most specific segments (anterior, anteroseptal, and all apical segments except the infero-apical) correspond to LAD but no segment can be exclusively attributed to the RCA. Inferoseptal segments can be attributed to LAD or RCA, inferior and inferolateral segments to RCA or LCX, and mid-anterolateral segment to LAD or LCX.

Introduction

Standard models of left ventricular segmentation have been used to facilitate a more detailed analysis of regional left ventricular function and perfusion. The left ventricular segmentation systems adopted in these models show an enormous range of variability, ranging between nine and 64 segments,[1–13] and make difficult to compare between different studies. The last recommendation of the American Heart Association suggests the use of the 17-myocardial segment model for all cardiac imaging modalities.[14] Even assuming that there is anatomic variability these segments were assigned to one of the three major coronary arteries.

Extent of hypoperfused myocardium in single-photon emission computed tomographic (SPECT) images with technetium-labelled compounds obtained during percutaneous transluminal coronary angioplasty (PTCA) balloon occlusion have been compared with those obtained during exercise and dipyridamole studies.[15–20] This procedure is based on the absence of redistribution of the ^{99m}Tc-compounds, which makes it possible to obtain a delayed image of the myocardial situation at the time of injection. However, none of the previous studies have considered this method to assign the different segments to the three major coronary arteries.

The aim of the present study is to analyse the correspondence of the 17 left ventricular myocardial segments with each coronary artery by myocardial perfusion SPECT studies with technetium-labelled marked compounds during total occlusion in the course of PTCA in patients with single-vessel disease.

Methods

Patient population

The study consisted of 50 consecutive patients (five women; mean age, 59.3 ± 10.8) without previous myocardial infarction, who underwent elective single PTCA by the same operator for single-vessel disease (stenosis >50%) depending on Nuclear Medicine Department availability. Three patients with evidence of collaterals were excluded. All patients were recruited at Hospital Universitari

* Corresponding author. Tel: +34 93 2746100 ext. 6681; fax: +34 93 2746063.
E-mail address: jcandell@vhebron.net

Vall d'Hebron of Barcelona, and Emory University provided quantitative tools to evaluate the images. The indications for coronary angioplasty were either unstable angina ($n = 22$) or exertional angina ($n = 28$). All patients had normal baseline electrocardiograms, normal rest myocardial perfusion SPECT, and received cardiac medications within 12 h of angioplasty; these included calcium channel antagonists in 27 patients, nitrates in 32, and adrenergic blocking agents in 23.

Patients were divided into three groups according to the balloon occlusion site: 24 patients in the left anterior descending (LAD) group, 15 patients in the right coronary artery (RCA) group, and 11 patients in the left circumflex (LCX) coronary arteries group. The study complies with the Declaration of Helsinki and was approved by the Ethics Committee of the hospital, and all patients signed informed consent.

Angiography and angioplasty

Coronary arteriography was performed using one of two Philips systems, Optimus M200 (biplane) or Integris (single plane). In all cases, a field of view of 17.8 cm was used, and the source-to-image intensifier distance was measured. According to our current practise, evaluation of stenosis severity was visually defined by the operator performing the procedure and was agreed usually with the patient's cardiologist or with some other interventional cardiologist. All stenoses included in the study were localized in proximal or mid-segments of main epicardial arteries. Localization of stenoses was defined as follows: proximal LAD when previous to the first septal or diagonal branch, mid-LAD from the first septal–diagonal branch to just before a distal diagonal branch, proximal LCX as previous to the obtuse marginal branch takeoff, mid-LCX from the obtuse marginal branch to a second marginal or posterolateral, proximal RCA as previous to the acute marginal, and mid-RCA from the acute marginal to the posterior descending takeoff. All patients received aspirin and ticlopidine at least 24 h before angioplasty. After intracoronary nitroglycerin injection, two orthogonal views were obtained. The views were selected to better define the degree of stenosis, to assess collateral flow, and to widely display the coronary tree affected by the flow limitation. The balloon catheter was passed via the femoral artery over a steerable guide wire under fluoroscopy and inflated across the coronary lesion. After 10–15 s of balloon inflation, 20–25 mCi of ^{99m}Tc-labelled compound was injected into a peripheral intravenous tubing and inflation was maintained at least 90 s to allow time for ^{99m}Tc-agent compound myocardial distribution. After that, further balloon inflations or stent deployments were performed to achieve revascularization to the myocardium.

SPECT acquisition, processing, and analysis

Once the angiographic study concluded, ~60 min after administering the ^{99m}Tc-labelled compound (32 patients with tetrofosmin and 18 with methoxyisobutyl isonitrile), the patients were transferred to the Nuclear Medicine Department to obtain the corresponding radionuclide scan at the time of the occlusion. Tomographic imaging was performed with a single-head gamma camera (Elscint SP4, Haifa) set for 140 keV photo peak with a 20% window. The acquisition was taken with a high-resolution collimator in a 64×64 matrix, with an enlargement factor 1.2 and 6.9 mm pixel size. Sixty projections (25 s/projection) were acquired using a semi-circular orbit starting at 30° right anterior oblique. Reconstructions were performed with a Butterworth filter of critical frequency 0.4 cycle/cm and an order of 5, and short-axis, horizontal long-axis, and vertical long-axis were obtained according to the current recommendations.[21] A polar map presentation was then generated from short-axis slices. No attenuation or scatter correction was used. Before reconstruction, all studies were corrected for non-uniformity with a 300 million counts matrix, obtained weekly from a ^{99m}Tc flood source.

The size of the defect was calculated using a threshold of 50%. Such cutoff value was derived from a previous validation of our gamma camera system using the Mayo Clinic phantom model[22] and had been previously used in clinical studies.[23] The extent of perfusion defect was quantified as a percentage of the entire left ventricular surface on polar map (binarized picture normal/abnormal) as shown in *Figure 1*. The extension of hypoperfused myocardium for each group was obtained by overlapping the maximum contour of each patient and transferred to a polar map of the 17 segments[14] and assigned to the three major coronary arteries. A segment was assigned to a given artery if the area at risk involved at least 25% of its surface.

Statistical analysis

Sensitivity, specificity, and predictive accuracy, and their 95% confidence intervals, were calculated for the diagnosis of LAD, RCA, and

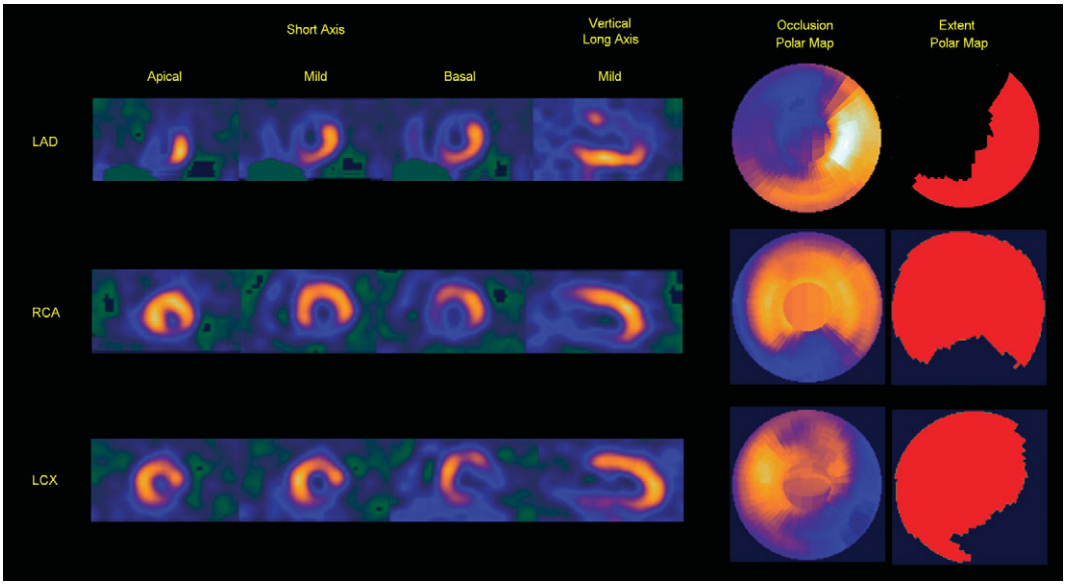

Figure 1 Examples of hypoperfused regions in tomographic slices and in the polar maps corresponding to the occlusion of LAD artery, RCA, and LCX artery. Black territory in the blackout polar map corresponds to the extent of myocardium with <50% of uptake with respect to the maximal left ventricular uptake.

LCX occlusions in segments supplied by more than one coronary artery. The χ^2 test was used to compare these results, and Fischer's exact test was used when less than five patients were expected in any subgroup. Data for continuous variables are described as mean $\pm$ SD, and categorical data were expressed as proportions. Unpaired *t*-test was used to compare the average extent of the hypoperfused region of LAD, RCA, and LCX groups. A *P*-value <0.05 was considered statistically significant. All *P*-values were two-sided. No adjustment for multiple comparisons was made.

Results

Coronary arteriography

No patient had complications during the percutaneous revascularization procedure. PTCA was performed in only one artery per patient by the same operator. No regions in the territory of the occluded vessel showed hypokinaesia, akinaesia, or diskinaesia before PTCA. No qualitative evidence of collateral circulation was observed in any patient.

In the LAD group (11 with proximal stenosis and 13 with mid-stenosis), 18 patients had a dominant RCA, five patients had a dominant LCX, and one patient had balanced coronary circulation. The LAD went around the apex to reach infero-apical region in 12 out of 24 patients of this group. In four patients, mild stenosis of LCX was observed. The left ventricular ejection fraction (LVEF), calculated by contrast ventriculography, was $70.1 \pm 8.2\%$. In the RCA group (nine with proximal stenosis and six with mid-stenosis), all patients had a dominant RCA. The RCA supplied the infero-apical region in seven out of 15 patients of this group. In three patients, mild stenosis of LCX (two) and LAD (one) was observed. The LVEF was $73.1 \pm 11.7\%$. In the LCX group (eight with proximal stenosis and three with mid-stenosis), nine patients had a dominant RCA, one had a dominant LCX, and one patient had balanced coronary circulation. In one patient, mild stenosis of LAD was observed. The LVEF was $72.6 \pm 11.1\%$.

Myocardial perfusion SPECT

The maximal extent of hypoperfused myocardium for each group in the polar map is shown in *Figure 2A* and the number of patients in whom each segment was involved is shown in *Figure 2B*.

According to the maximal contour of hypoperfused myocardium of each group, the correspondence between 17 myocardial segments and each coronary artery is shown in *Figure 3*. Basal anterior (1), basal anteroseptal (2), mid-anterior (7), mid-anteroseptal (8), apical anterior (13), apical septal (14), apical lateral (16), and apex (17) segments corresponded to LAD (specificity, 100%). Basal anterolateral (6) segment corresponded to LCX (specificity, 100%).

Basal inferoseptal (3), mid-inferoseptal (9), and apical inferior (15) segments could correspond to LAD or RCA. Basal inferior (4), basal inferolateral (5), mid-inferior (10), and mid-inferolateral (11) segments could correspond to RCA or LCX, and mid-anterolateral (12) segment could correspond to LAD or LCX. *Table 1* shows the diagnostic accuracy in the segments supplied by more than one coronary artery. Sensitivity, specificity, and negative predictive accuracy in segment 5 were significantly higher for LCX when compared with RCA.

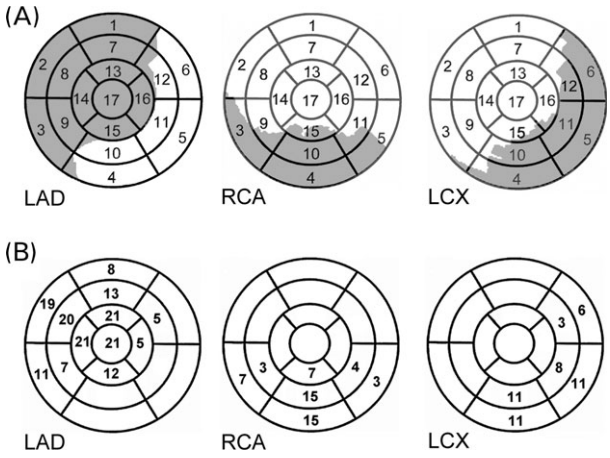

Figure 2 (*A*) Maximal extent of hypoperfused myocardium for LAD group, RCA group, and LCX group overlapped in the polar map of 17 segments. (*B*) Number of patients with involvement of each segment.

An additional analysis, including adjacent segments, demonstrated that the coronary artery territory can be more accurately localized. Thus, the inferior and infero-lateral segments can belong to either the RCA or the LCX artery. However, if the anterolateral segments are also involved in a given patient, the distribution appears to be more specific for the LCX, whereas if the inferoseptal segments are involved, the distribution appears to be more specific for the RCA. Similarly, the inferoseptal segment can belong to either the LAD or the RCA, but if the adjacent inferior segments are also involved, the territory appears to be more specific for the LAD. Likewise, the infero-apical segment can belong to either the RCA or the LAD, but if the other apical segments are involved, the territory appears to be more specific for the LAD, whereas if the inferior segments at the mid- and basal levels are involved, the distribution appears to be more specific for the RCA.

The average extent of the hypoperfused region was significantly greater for the LAD group (mean extent, $49.8 \pm 10.3\%$; range 35–67%) when compared with RCA group (mean extent, $20.3 \pm 7.6\%$; range 8.3–35.0%) ($P < 0.0001$, 95% confidence interval 23.3–35.7) and LCX group (mean extent, $21.3 \pm 10.8\%$; range 10.2–30.0%) ($P < 0.0001$, 95% confidence interval 20.7–36.2). The mean extents of RCA and LCX hypoperfused regions were not significantly different ($P = 0.784$, 95% confidence interval -6.4–8.4).

Discussion

A 17-segment model of the left ventricle has been recommended for myocardial perfusion SPECT, echocardiography, computed tomography, and magnetic resonance imaging as an optimally weighted approach for the visual interpretation of regional left ventricular abnormalities.[14] Although, as recommended in these guidelines, there is a variability in the coronary blood supply to myocardial segments, the model was believed to be appropriate for assigning individual segments to specific coronary artery territories,[15] and a map of this correspondence is included in the guidelines.[14] The authors pointed out that the

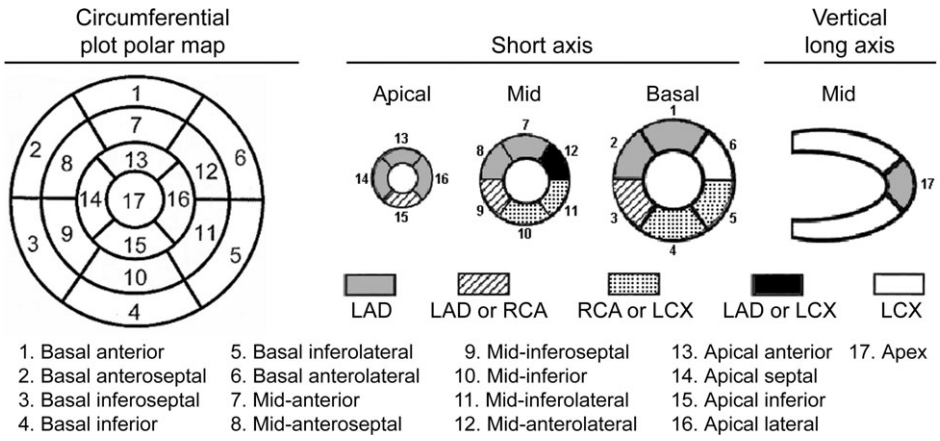

Figure 3 Correspondence of left ventricular 17 myocardial segments with each coronary artery according to our results.

greatest variability in myocardial blood supply occurs at the apical segment 17, which can be supplied by any of the three arteries. Segments 1, 2, 7, 8, 13, and 17 are assigned to the LAD coronary artery distribution. Segments 3, 4, 9, and 10 are assigned to the RCA when it is dominant. Segments 5, 6, 11, 12, and 16 generally are assigned to the LCX artery.

Myocardial perfusion SPECT is frequently performed before coronary angiography to know localization and extent of jeopardized myocardium, and after angiography, to evaluate the haemodynamic significance of non-critical stenoses.[24–27] Thus, misassignment of myocardial segments could alter the perception concerning the coronary arteries involved. Coronary occlusion during PTCA provides an *in vivo* model for examining the effects of acute myocardial ischaemia on ventricular function and perfusion.[15–20] ^{99m}Tc- compounds are perfusion agents, which accumulate in the myocardium in proportion to regional distribution of coronary blood flow at the time of injection with minimal redistribution. Experimentally, the jeopardized myocardium assessed following their injection during coronary artery occlusion correlates with initial area at risk and final infarct size.[21,28,29] Clinical studies have shown that the myocardial area at risk can be imaged after injection of these ^{99m}Tc-compounds before thrombolytic therapy in patients with acute myocardial infarction.[30] It has also been shown that myocardial perfusion SPECT is able to detect brief episodes of ischaemia caused by complete occlusion of a coronary artery during PTCA.[31,32] ^{99m}Tc-sestamibi and ^{99m}Tc-tetrofosmin would therefore be used to demonstrate the myocardial area supplied by a coronary artery, if injected during prolonged PTCA balloon occlusion. Using this methodology, we have previously reported the extent of the ischaemic territory corresponding to the occlusions of LAD, RCA, and CX[33] and validated a three-dimensional fusion of coronary arteries with myocardial perfusion distributions.[34] Moreover, good reproducibility of the different tomographic methods quantifying myocardial area at risk during coronary artery occlusion has been reported.[20] However, no studies have been designed for the assignment of each of the 17 left ventricular segments to each one of the three major coronary arteries.

The purpose of the present study is to evaluate the correspondence between coronary artery distribution and myocardial perfusion defects in the 17 myocardial segments of left ventricle obtained during total occlusion of each one of the three major coronary arteries in the course of PTCA in patients with single-vessel disease. In contrast with the generally accepted assignment of coronary artery territories, our results show that only nine segments correspond to only one coronary artery. Eight segments correspond to LAD: basal anterior (1), basal anteroseptal (2), mid-anterior (7), mid-anteroseptal (8), apical anterior (13), apical septal (14), apical lateral (16), and apex (17) and one to CX: basal anterolateral (6). Basal inferoseptal (3), mid-inferoseptal (9), and apical inferior (15) segments can correspond to LAD or RCA. Basal inferior (4), basal inferolateral (5), mid-inferior (10), and mid-inferolateral (11) segments can correspond to RCA or LCX and mid-anterolateral (12) segment can correspond to LAD or LCX. Although the greatest superposition in myocardial blood supply occurs in the inferolateral region corresponding to RCA and LCX territories, superposition of LAD and RCA territories also occurs at the level of inferoseptal region. Mid-anterolateral segment is the unique conflictive territory between LAD and LCX. Despite these considerations, an additional analysis that includes adjacent segments can help to clarify the role of SPECT imaging for localization of disease. This explains why myocardial perfusion SPECT can identify angiographic culprit lesion localization in 85% of cases,[24,35] while mistakenly predicts additional vessel involvement in 29% of cases.[35]

Segmental analysis of myocardial perfusion studies is based on certain assumptions concerning coronary anatomy. The nearly universal approach is to assign the anterior wall and septum to the LAD, the lateral wall to the LCX, and the inferior wall to the RCA. However, there is no consensus on the exact borders of each vascular territory as evidenced by the significant variation in quantitative polar maps. These differences may be explained by the normal variability of the coronary anatomy.[36,37] The most frequent variation is the origin of the posterior descending artery. The RCA is dominant in $>$70% of hearts. Other terminal branches of the RCA and LCX, called posterolateral branches, supply a variable amount of the inferior wall. The great variability in blood supply to the inferior and lateral walls is reflected in our study. The inferior segments are almost always assumed to be supplied by the RCA. In our study, all 11 patients with LCX disease had involvement of

Table 1 Diagnostic accuracy of myocardial perfusion SPECT for segments supplied by more than one artery

	Sensitivity (95% CI)	Specificity (95% CI)	Predictive accuracy (95% CI)	Sensitivity (95% CI)	Specificity (95% CI)	Predictive accuracy (95% CI)
LAD vs. RCA						
	RCA			LAD		
Segment 3	46 (26–67)	53 (27–79)	49 (32–65)	47 (21–73)	54 (33–74)	51 (35–68)
Segment 9	29 (13–51)	80 (52–96)	49 (32–65)	20 (4–48)	71 (49–87)	51 (35–68)
Segment 15	50 (29–71)	53 (27–79)	51 (35–68)	47 (21–73)	50 (29–71)	49 (32–65)
RCA vs. LCX						
	LCX			RCA		
Segment 4	100 (78–100)	0 (0–28)	58 (37–77)	100 (72–100)	0 (9–22)	42 (23–63)
Segment 5	20 (4–48)	0 (0–28)	12 (2–30)	100 (72–100)	80 (52–96)	89 (70–98)
Segment 10	100 (78–100)	0 (9–28)	58 (37–77)	100 (72–100)	0 (0–22)	42 (23–63)
Segment 11	27 (8–55)	27 (6–61)	27 (12–48)	73 (39–94)	73 (45–92)	73 (52–88)
LAD vs. LCX						
	LCX			LAD		
Segment 12	21 (7–42)	73 (39–44)	37 (21–55)	27 (6–61)	79 (58–93)	63 (45–78)

CI, confidence interval.

the inferior segments, and in patients with LCX disease, involvement of inferior segments was more common than involvement of the anterolateral segments. The finding of an inferior perfusion defect extending to the mid-septum in a patient with RCA stenosis is more unusual. Although the septum is supplied by branches from both the LAD and the posterior descending artery, anterior septal branches are longer than posterior septal branches. The inferior septum is commonly assigned to the distribution of the RCA. However, only half of the patients with RCA disease had involvement of the inferior septum. Conversely, approximately half of the patients with LAD disease also had involvement of the inferior septum. The apical portion, as our study reveals, is almost exclusively supplied by branches of the LAD. The supply of the apical segments (nos 13–17) is dominated by the LAD. The RCA was the only vessel other than LAD to supply any of the apical segments (segment no. 15). Even this segment is more commonly supplied by the LAD than the RCA. Many nuclear cardiologists and clinicians believe that the supply of the apex can be subdivided into the individual coronary territories, but this assumption is incorrect. The LAD is the primary vessel supplying the apex in the vast majority of patients. Another source of variability is the length and termination point of the LAD; the termination point is distal to the apex in 60–82% of cases. Thus, the LAD perfuses the infero-apical segment in the majority of hearts. These data are consistent with our observations.

The data of this study are based on relatively few patients, particularly in view of the great variability of the coronary tree. This may explain, for instance, that the apex (segment no. 17) and the apicolateral regions (segment no. 16) are 100% specific for the LAD. In addition to the small number of patients, some limitations of this study need to be kept in mind. The presence of stenosis $<$70% in not occluded arteries could overestimate the limits of the myocardium attributed to the studied coronary arteries. As in other studies oriented to quantify the extent of infarction, we selected 50% isocontour as the cutoff value to quantify the extent of jeopardized myocardium. Additional lesions should not influence this extent in rest images. The search for collateral vessels was performed only on the basis of detecting spontaneously visible coronary collaterals during coronary angiography. Although this approach does not totally exclude the presence of coronary collateral circulation, accurate techniques for detecting collateral flow were not considered because of the complexity (and thus time and risk) that they would have added to the angioplasty procedure in this population of patients with a single-coronary lesion. In addition, adjustment for attenuation artefacts was not implemented in our study and area of myocardium at risk could be increased in inferior and anterior regions because of diaphragmatic and breast interposition, respectively, but 90% of our patients were male.

In conclusion, the most specific segments (anterior, anteroseptal, and all apical segments except the infero-apical) correspond to LAD, but no segment can be exclusively attributed to the RCA. Inferoseptal segments can be attributed to LAD or RCA, inferior and inferolateral segments can be attributed to RCA or LCX, and mid-anterolateral segment can be attributed to LAD or LCX.

Acknowledgement

This study was partially funded by a grant from the 'Redes temáticas de investigación cooperativa. Instituto Carlos III (Red C03/01, RECAVA)'.

Conflict of interest: none declared.

References

1. Heller GV, Stowers SA, Hendel RC, Herman SD, Daher E, Ahlberg AW, Baron JM, Mendes de Leon CF, Rizzo JA, Wackers FJ. Clinical value of acute rest technetium-99 m tetrofosmin tomographic myocardial perfusion imaging in patients with acute chest pain and nondiagnostic electrocardiograms. *J Am Coll Cardiol* 1998;**31**:1011–1017.
2. Berman DS, Kiat H, Friedman JD, Wang FP, van Train K, Matzer L, Maddahi J, Germano G. Separate acquisition rest thallium-201/stress technetium-99 m sestamibi dual-isotope myocardial perfusion single-photon emission computed tomography: a clinical validation study. *J Am Coll Cardiol* 1993;**22**:1455–1464.
3. Hachamovitch R, Berman DS, Shaw LJ, Kiat H, Cohen I, Cabico JA, Friedman J, Diamond GA. Incremental prognostic value of myocardial perfusion single photon emission computed tomography for the prediction of cardiac death: differential stratification for risk of cardiac death and myocardial infarction. *Circulation* 1998;**97**:535–543.
4. Taillefer R, DePuey EG, Udelson JE, Beller GA, Benjamin C, Gagnon A. Comparison between the end-diastolic images and the summed images of gated 99mTc-sestamibi SPECT perfusion study in detection of coronary artery disease in women. *J Nucl Cardiol* 1999;**6**:169–176.
5. Vaduganathan P, He ZX, Vick GW, Mahmarian JJ, Verani MS. Evaluation of left ventricular wall motion, volumes, and ejection fraction by gated myocardial tomography with technetium 99 m-labeled tetrofosmin: a comparison with cine magnetic resonance imaging. *J Nucl Cardiol* 1999;**6**:3–10.
6. Eisner RL, Martin SE, Leon AR, Schmarkey LS, Worthy MA, Chu TH, Patterson RE. Inhomogeneity of gated and ungated SPECT technetium-99 m-sestamibi bull's-eyes in normal dogs: comparison with thallium-201. *J Nucl Med* 1993;**34**:281–287.
7. Dilsizian V, Perrone-Filardi P, Cannon RO, Freedman NM, Bacharach SL, Bonow RO. Comparison of exercise radionuclide angiography with thallium SPECT imaging for detection of significant narrowing of the left circumflex coronary artery. *Am J Cardiol* 1991;**68**:320–328.
8. Kaul S, Senior R, Dittrich H, Raval U, Khattar R, Lahiri A. Detection of coronary artery disease with myocardial contrast echocardiography: comparison with 99mTc-sestamibi single photon emission computed tomography. *Circulation* 1997;**96**:785–792.
9. Marwick T, D'Hondt AM, Baudhuin Twillemart B, Wijns W, Detry JM, Melin J. Optimal use of dobutamine stress for the detection and evaluation of coronary artery disease: combination with echocardiography or scintigraphy, or both? *J Am Coll Cardiol* 1993;**22**:159–167.
10. Gregoire J, Theroux P. Detection and assessment of unstable angina using myocardial perfusion imaging: comparison between technetium-99 m sestamibi SPECT and 12-lead electrocardiogram. *Am J Cardiol* 1990;**66**:42E–46E.
11. Danias PG, Ahlberg AW, Clark BA, Messineo F, Levine MG, McGill CC, Mann A, Clive J, Dougherty JE, Waters DD, Heller GV. Combined assessment of myocardial perfusion and left ventricular function with exercise technetium-99 m sestamibi gated single-photon emission computed tomography can differentiate between ischemic and nonischemic dilated cardiomyopathy. *Am J Cardiol* 1998;**82**:1253–1258.
12. Kwok JM, Christian TF, Miller TD, Hodge DO, Gibbons RJ. Identification of severe coronary artery disease in patients with a single abnormal coronary territory on exercise thallium-201 imaging: the importance of clinical and exercise variables. *J Am Coll Cardiol* 2000;**35**:335–344.
13. Brown KA, Heller GV, Landin RS, Shaw LJ, Beller GA, Pasquale MJ, Haber SB. Early dipyridamole (99 m)Tc-sestamibi single photon emission computed tomographic imaging 2 to 4 days after acute myocardial infarction predicts in-hospital and postdischarge cardiac events: comparison with submaximal exercise imaging. *Circulation* 1999;**100**:2060–2066.
14. Cerqueira MD, Weissman NJ, Dilsizian V, Jacobs AK, Kaul S, Laskey WK, Pennell DJ, Rumberger JA, Ryan T, Verani MS. Standardized myocardial segmentation and nomenclature for tomographic imaging of the heart. A Statement for Healthcare Professionals from the Cardiac Imaging Committee of the Council on Clinical Cardiology of the American Heart Association. *Circulation* 2002;**105**:539–542.
15. Gallik DM, Obermueller SD, Swarna US, Guidry JW, Mahmarian JJ, Verani MS. Simultaneous assessment of myocardial perfusion and left ventricular function during transient coronary occlusion. *J Am Coll Cardiol* 1995;**25**:1529–1538.
16. Wiske PS, Palacios I, Block PC, O'Gara P, Strauss HW, Okada RD, Boucher CA. Assessment of regional myocardial perfusion with thallium imaging during transient left anterior coronary arterial occlusion during angioplasty. *Am J Cardiol* 1986;**57**:1083–1087.
17. Borges-Neto S, Puma J, Jones RH, Sketch MH, Stack R, Hanson MW, Coleman RE. Myocardial perfusion and ventricular function measurements during total coronary artery occlusion in humans. A comparison with rest and exercise radionuclide studies. *Circulation* 1994;**89**:278–284.
18. Borges-Neto S, Watson JE, Miller MJ. Tc-99 m sestamibi cardiac SPECT imaging during coronary artery occlusion in humans: comparison with dipyridamole stress studies. *Radiology* 1996;**198**:751–754.
19. Persson E, Palmer J, Pettersson J, Warren SG, Borges-Neto S, Wagner GS, Pahlm O. Quantification of myocardial hypoperfusion with 99 m Tc-sestamibi in patients undergoing prolonged coronary artery balloon occlusion. *Nucl Med Commun* 2002;**23**:219–228.
20. Ceriani L, Verna E, Giovanella L, Bianchi L, Roncari G, Tarolo GL. Assessment of myocardial area at risk by technetium-99 m sestamibi during coronary artery occlusion: comparison between three tomographic methods of quantification. *Eur J Nucl Med* 1996;**23**:31–39.
21. Committee on Advanced Cardiac Imaging and Technology, Council on Clinical Cardiology, American Heart Association; Cardiovascular Imaging Committee, American College of Cardiology; and Board of Directors, Cardiovascular Council, Society of Nuclear Medicine. Standardization of cardiac tomographic imaging. *Circulation* 1992;**86**:338–339.
22. O'Connor MK, Gibbons RJ, Juni JE, O'Keefe J, Ali A. Quantitative myocardial SPECT for infarct sizing: feasibility of a multicenter trial evaluated using a cardiac phantom. *J Nucl Med* 1995;**36**:1130–1136.
23. Schömig A, Kastrati A, Dirschinger J, Mehilli J, Schricke U, Pache J, Martinoff S, Neumann FJ, Schwaiger M, for the Stent versus Thrombolysis for Occluded Coronary Arteries in Patients with Acute Myocardial Infarction Study Investigators. Coronary stenting plus platelet glycoprotein IIb/IIIa blockade compared with tissue plasminogen activator in acute myocardial infarction. *N Engl J Med* 2000;**343**:385–391.
24. Candell-Riera J, Santana-Boado C, Castell-Conesa J, Aguadé-Bruix S, Olona-Cabases M, Domingo E, Permanyer-Miralda G, Soler-Soler J. Culprit lesion and jeopardized myocardium: correlation between coronary angiography and single photon emission computed tomography. *Clin Cardiol* 1997;**20**:345–350.
25. Abe M, Tomiyama H, Yoshida H, Doba N. Diastolic fractional flow reserve to assess the functional severity of moderate coronary artery stenoses: comparison with fractional flow reserve and coronary flow velocity reserve. *Circulation* 2000;**102**:2365–2370.
26. Chamuleau S, Meuwissen M, van Eck-Smit BLF, Koch KT, de Jong A, de Winter RJ, Schotborgh CE, Bax M, Verberne HJ, Tijssen JGP, Piek JJ. Fractional flow reserve, absolute and relative coronary blood flow velocity reserve in relation to the results of technetium-99 m sestamibi single-photon emission computed tomography in patients with two-vessel coronary artery disease. *J Am Coll Cardiol* 2001;**37**:1316–1322.
27. Briguori C, Anzuini A, Airoldi F, Gimelli G, Nishida T, Adamian M, Corvaja N, Di Mario C, Colombo A. Intravascular ultrasound criteria for the assessment of the functional significance of intermediate coronary artery stenoses and comparison with fractional flow reserve. *Am J Cardiol* 2001;**87**:136–141.
28. Sinusas AJ, Trautman KA, Bergin JD, Watson DD, Ruiz M, Smith WH, Beller GA. Quantification of area at risk during coronary occlusion and degree of myocardial salvage after reperfusion with technetium-99 m methoxyisobutil isonitril. *Circulation* 1990;**82**:1424–1437.
29. De Coster PM, Wijns W, Cauwe F, Robert A, Beckers C, Melin JA. Area-at-risk determination by technetium-99 m-hexakis-2-methoxyisobutil isonitrile in experimental reperfused myocardial infarction. *Circulation* 1990;**82**:2152–2162.
30. Gibbons RJ, Verani MS, Behrenbeck T, Pellikka PA, O'Connor MK, Mahmarian JJ, Chesebro JH, Wackers FJ. Feasibility of tomographic 99mTc-hexakis-2-methoxi-2-methylpropyl-isonitrile imaging for the assessment of myocardial area at risk and the effect of treatment in acute myocardial infarction. *Circulation* 1989;**80**:1277–1286.
31. Pfisterer M, Müller-Brand J, Spring P, Bassignana V, Kiowski W. Assessment of the extent of jeopardized myocardium during acute coronary artery occlusion followed by reperfusion in man using technetium-99 m isonitrile imaging. *Am Heart J* 1991;**122**:7–12.

32. Braat SH, DeSwart H, Rigo P, Koppejan L, Heidendal GAK, Wellens HJJ. Value of technetium MIBI to detect short lasting episodes of severe myocardial ischemia and to estimate the area at risk during coronary angioplasty. *Eur Heart J* 1991;**12**:30–33.
33. Pereztol-Valdés O, Candell-Riera J, Oller-Martínez G, Aguadé-Bruix S, Castell-Conesa J, Angel J, Soler-Soler J. Localización y cuantificación del área en riesgo mediante tomografía computarizada por emisión de fotones simples de perfusión miocárdica durante la oclusión arterial coronaria. *Rev Esp Cardiol* 2004;**57**:635–643.
34. Faber TL, Santana CA, Garcia EV, Candell-Riera J, Folks RD, Peifer JW, Hopper A, Aguadé S, Angel J, Klein JL. Three-dimensional fusion of coronary arteries with myocardial perfusion distributions: clinical validation. *J Nucl Med* 2004;**45**:745–753.
35. Segall GM, Atwood E, Botvinick EH, Dae MW, Lucas JR. Variability of normal coronary anatomy: implications for the interpretation of thallium-SPECT myocardial perfusion images in single vessel disease. *J Nucl Med* 1995;**36**:944–951.
36. Paulin S. Normal coronary anatomy. In: Abrams HL, ed. *Coronary Arteriography. A Practical Approach*. Boston: Little, Brown and Company; 1983. p127–174.
37. Alderman EL, Stadius M. The angiographic definitions of the bypass angioplasty revascularization investigation. *Coron Artery Dis* 1992;**3**:1189–1207.

Clinical vignette

doi:10.1093/eurheartj/ehi514
Online publish-ahead-of-print 24 October 2005

Transthoracic echocardiography of Hodgkin lymphoma in the upper anterior mediastinum causing compression of the great vessels

Alexander Nossikoff*, Rumiana Radoslavova, Simeon Dimitrov, and Stefan Denchev

Department of Internal Medicine, Clinic of Cardiology, University Hospital Alexander, G. Sofijski str. 1, 1431 Sofia, Bulgaria

* Corresponding author. *E-mail address*: alexanderbul@yahoo.com

A 37-year-old man with pulsus paradoxus, non-productive cough, and fatigue was referred to our institution for diagnostic workup. A transthoracic echocardiography was performed, revealing pericardial effusion (PE) with right atrial compression and bilateral pleural effusions (PLE) with fibrinous strands (Panel A). High parasternal oblique scan revealed a huge mass (maximum antero-posterior diameter, 13.9 cm), with 'parenchymatous' texture (LY) in the upper anterior mediastinum displacing the aorta (AO) and pulmonary artery (PA) posteriorly and surrounding them (Panel B).

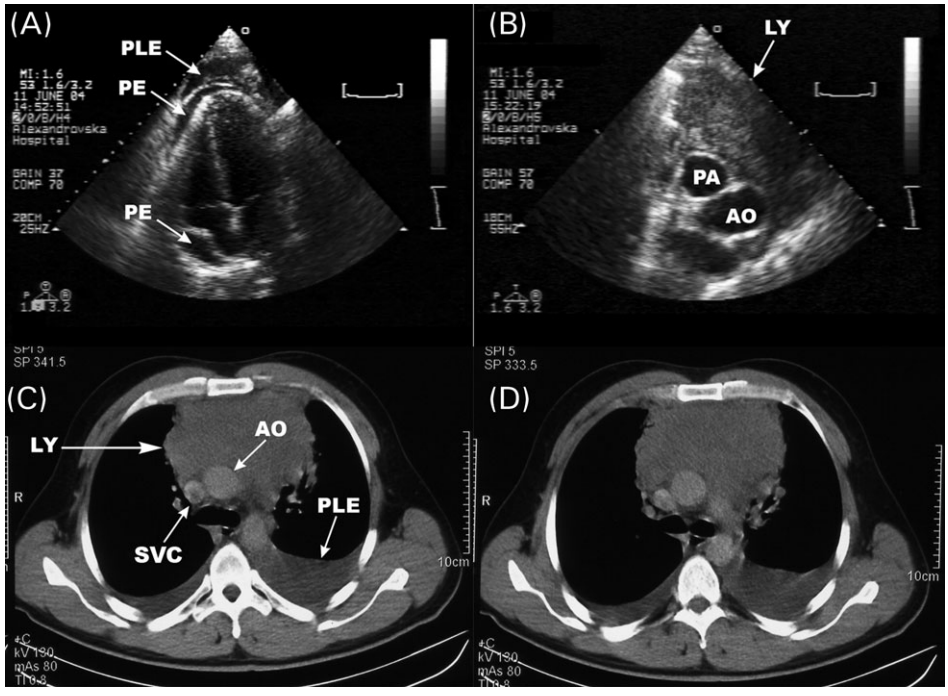

Contrast-enhanced CT of thorax and abdomen was performed, confirming the findings from echocardiography revealing also displacement of superior vena cava (SVC) (Panels C and D). No other sites of involvement were seen. Transthoracic true-cut needle biopsy was performed. Histology confirmed the preliminary diagnosis of Hodgkin lymphoma.

The patient was referred to chemotherapy and was serially followed up. After the first chemotherapy regimen, the pleural and pericardial effusions disappeared and the patient was with stable haemodynamics and had no complaints of cough. After the complete uneventful chemotherapy course, the antero-posterior diameter of the mass decreased to 3.9 cm. The patient is fully asymptomatic and is referred to radiotherapy.

See online supplementary material available at *European Heart Journal* online for a colour version of the figure.